Hellenic Journal of Cardiology xxx (xxxx) xxx

Contents lists available at ScienceDirect

Hellenic Journal of Cardiology

journal homepage: http://www.journals.elsevier.com/hellenic-journal-of-cardiology/

Original Article

A novel diagnostic tool to identify atrial endo-epicardial asynchrony using signal fingerprinting

Lu Zhang [1], Mathijs S. van Schie [1], Paul Knops [1], Yannick J.H.J. Taverne [2], Natasja M.S. de Groot [1, 3, *]

[1] Department of Cardiology, Erasmus Medical Center, Rotterdam, the Netherlands
[2] Translational Cardiothoracic Surgery Research Lab, Department of Cardiothoracic Surgery, Erasmus Medical Center, Rotterdam, the Netherlands
[3] Department of Microelectronics, Signal Processing Systems, Faculty of Electrical Engineering, Mathematics and Computer Sciences, Delft University of Technology, Delft, the Netherlands

ARTICLE INFO

Article history:
Received 11 April 2023
Received in revised form
4 June 2023
Accepted 18 July 2023
Available online xxx

Keywords:
Endo-epicardial asynchrony
Asynchrony Fingerprinting Score
Low-voltage areas
Fractionation
unipolar electrograms

ABSTRACT

Objective: Patients with persistent atrial fibrillation (AF) have more electrical endo-epicardial asynchrony (EEA) during sinus rhythm (SR) than patients without AF. Prior mapping studies indicated that particularly unipolar, endo- and/or epicardial electrogram (EGM) morphology may be indicators of EEA. This study aim to develop a novel method for estimating the degree of EEA by using unipolar EGM characteristics recorded from either the endo- and/or epicardium.
Methods: Simultaneous endo-epicardial mapping during sinus rhythm was performed in 86 patients. EGM characteristics, including unipolar voltages, low-voltage areas (LVAs), potential types (single, short/long double and fractionated potentials: SP, SDP, LDP and FP) and fractionation duration (FD) of double potentials (DP) and FP were compared between EEA and non-EEA areas. Asynchrony Fingerprinting Scores (AFS) containing quantified EGM characteristics were constructed to estimate the degree of EEA.
Results: Endo- and epicardial sites of EEA areas are characterized by lower unipolar voltages, a higher number of LDPs and FPs and longer DP and FP durations. Patients with AF have lower potential voltages in EEA areas, along with alterations in the potential types. The EE-AFS, containing the proportion of endocardial LVAs and FD of epicardial DPs, had the highest predictive value for determining the degree of EEA (AUC: 0.913). Endo- and epi-AFS separately also showed good predictive values (AUC: 0.901 and 0.830 respectively).
Conclusions: EGM characteristics can be used to identify EEA areas. AFS can be utilized as a novel diagnostic tool for accurately estimating the degree of EEA. These characteristics potentially indicate AF related arrhythmogenic substrates.

1. Introduction

Electrical asynchrony between the endo- and epicardium contributes to the perpetuation of atrial fibrillation (AF).[1,2] Several mapping studies have demonstrated that endo-epicardial asynchrony (EEA) occurs during AF and is associated with AF severity.[3-7] Even during sinus rhythm (SR), it has been demonstrated that EEA was more apparent in individuals with persistent AF than those without AF.[8] Recently, van der Does et al.[9] found that, although local endo-epicardial discrepancies in electrogram (EGM) fractionation occurred infrequently, fractionated EGMs could originate from areas of EEA. It was also shown that unipolar EGMs are more suitable for identifying EEA than bipolar EGMs.[10] These observations indicate that

Abbreviations: EED, endo-epicardial dissociation; EEA, endo-epicardial asynchrony; LVAs, low-voltage areas; SP, single potentials; SDP, short double potentials; LDP, long double potentials; FP, fractionated potentials; DP, double potentials; AFS, Asynchrony Fingerprinting Scores.

* Corresponding author. Prof. dr. N.M.S de Groot, Unit Translational Electrophysiology, Department of Cardiology Erasmus Medical Center, Dr. Molewaterplein 40, 3015GD, Rotterdam, the Netherlands. Tel.: +31-10-7035018; Fax: +31-10-7035258.
E-mail address: n.m.s.degroot@erasmusmc.nl (N.M.S. de Groot).
Peer review under responsibility of Hellenic Society of Cardiology.

https://doi.org/10.1016/j.hjc.2023.07.006

unipolar, endo- and/or epicardial EGM characteristics during SR may contain information on the presence of EEA. However, the EGM characteristics that can be used to accurately identify EEA remain unknown.

In this study, the hypothesis that specific atrial unipolar epi- and/or endocardial EGM characteristics reflect areas of EEA and estimate the degree of EEA was tested. For this purpose, simultaneous endo-epicardial mapping was conducted and EGM characteristics between EEA and non-EEA areas were compared. In addition, a novel diagnostic tool, the Asynchrony Fingerprinting Score (AFS), using quantified EGM characteristics for estimation of the degree of EEA was introduced.

2. Methods

2.1. Study population

The study population consisted of 86 patients undergoing elective open-heart surgery (coronary artery bypass surgery, valvular heart surgery or a combination of both) in the Erasmus Medical Center Rotterdam. Patient characteristics (e.g. age, medical history, cardiovascular risk factors) were obtained from the patient's medical record. This study was approved by the institutional medical ethical committee (MEC2015-373), and written informed consent was obtained from all patients.

2.2. Simultaneous endo-epicardial mapping of the right atrium

Simultaneous endo-epicardial high-resolution mapping was performed prior to extra-corporal circulation. A summary of the methodology is provided in supplemental Figure 1A and described in detail previously.[8] Two electrode arrays were used for simultaneous mapping of the epicardium and endocardium, each containing 128 (8 × 16) unipolar electrodes with a diameter of 0.45 mm and 2 mm interelectrode distance (IED). They were fixed on 2 bendable spatulas and were located on the exact opposite position of right atrial (RA) wall. After heparinization and arterial cannulation, the endocardial electrode array of spatula was introduced into the right atriotomy in which the venous canula will be inserted. The last row of electrodes of the endocardial spatula was introduced at least 1.5 cm into the RA to avoid overlap of the mapping area near the incision. To allow hemostatic measurements, the pursestring suture was secured. A temporal bipolar epicardial pacemaker wire was attached to the free wall as a reference electrode. An indifferent electrode was fixed to the subcutaneous tissue of the thoracic cavity. Simultaneous endo-epicardial mapping was performed at 3 different locations on the RA superior, mid and inferior free wall, as depicted in supplemental Figure 1A. EGMs were recorded for 5 seconds during stable sinus rhythm, including a surface electrocardiogram (ECG) lead, a calibration signal of 2 mV and 1000 ms and a bipolar reference EGM. Data were stored on a hard disk after sampling (1 kHz), amplification (gain 1000), filtering (bandwidth 0.5–400 Hz) and then analog to digital conversion (16 bits).

2.3. Mapping data analysis

Mapping data were semi-automatically analyzed using custom-made Python 3.8 software. Premature and aberrant beats were excluded. Areas of simultaneous activation were also excluded from analysis in order to avoid the inclusion of far-field potentials. All annotations were manually checked with a consensus of two investigators.

The steepest negative slope of a unipolar potential was annotated as local activation time (LAT) and used to compose color-coded activation maps.[11] As shown in the lower right panel of supplemental Figure 1, potentials were classified into 4 types according to their morphology: 1. single potentials (SP), consisting of one single negative deflection; 2. double potentials (DP): a. short double potentials (SDP) containing two deflections separated by <15 ms; b. long double potentials (LDP), containing two deflections separated by ≥15 ms and 3. fractionated potentials (FP) composed of more than three deflections. Fractionation duration (FD) was defined as the time difference (ms) between the first and last deflection of double potentials (DP: SDP+LDP) and FP. Potential voltage was defined as the peak-to-peak amplitude of the steepest deflection and low-voltage areas (LVAs) as recording sites from which potentials with voltages <1.0 mV were recorded.[12]

As shown in the upper right panel of supplemental Figure 1, endo-epicardial dissociation (EED) was determined by selecting the median of the LAT differences within the endo- and epicardial electrodes and its 8 surrounding electrodes from the opposite side.[8] When the EED exceeded 15 ms between every endo-epicardial electrode pair, as previously described, it was defined as endo-epicardial asynchrony (EEA).[8] The total amount of EEA for each patient was calculated as the proportion (EEA%) of the total mapping area during the entire recording period. Patients who have more than the 50th percentile of EEA% measured in the entire study population were defined as having a high-degree of EEA.

2.4. Statistical analysis

Normally distributed continuous variables were presented as mean ± standard deviation (SD) and skewed data were presented as median [25th, 75th percentile]. The Mann–Whitney U test or Kruskal-Wallis test was used to compare differences between groups of non-normally distributed data. Categorical data were presented as numbers and percentages and compared with the chi-squared test. Spearman correlations were performed to determine correlations between endo- and epicardial EGM characteristics. Spearman's correlation coefficients were categorized as weak (<0.4), moderate (0.4-0.6) or strong (>0.6). A p-value of <0.05 was considered statistically significant. Statistically significant variables were included in the multivariate logistic regression analysis for predicting a high amount of EEA. Statistical analyses were performed using Python (SciPy) and IBM SPSS Statistics version 26 (IBM Corp, Armonk, NY). *R* (4.2.1) software (rms, pROC and nomogram Formula package) was used to construct and visualize a nomogram as a tool for an Asynchrony Fingerprinting Score (AFS) and the receiver operator characteristic curve (ROC).

3. Results

3.1. Study population

Clinical characteristics of the study population (N = 86, age 67 [61–72] years, 68 male (79.1%)) are summarized in Table 1. Thirty-seven (43.0%) patients had a history of AF. Ischemic heart disease, valvular heart disease or combined ischemic and valvular heart disease were present in 43 (50.0%), 22 (25.6%), and 20 (23.3%) patients, respectively. Most patients used class II antiarrhythmic drugs (N = 59, 68.6%).

3.2. Mapping data

In the entire study population, a total of 1,641 (19 ± 7.5 per patient) heart beats were recorded during sinus rhythm (876 ± 190 ms). The resulting mapping locations consisted of 162,443 endocardial and 162,443 epicardial potentials.

As listed in Table 2, in every patient, endocardial voltages were lower than epicardial voltages (4.65 [3.15, 6.52] mV vs 7.01 [5.34,

Table 1
Baseline characteristics
Values are presented as N (%) or median [interquartile ranges].

Patients	86
Male	68 (79.1%)
Age (years)	67 [61 – 72]
BMI (kg/m^2)	27.9 [24.8 – 31.0]
Underlying heart disease	
iHD	43 (50.0%)
vHD	22 (25.6%)
cHD	20 (23.2%)
arrhythmia	1 (1.2%)
History of AF	37 (43.0%)
Paroxysmal	31 (36.0%)
Persistent	4 (4.7%)
Longstanding persistent	2 (2.3%)
Cardiovascular risk factors	
Hypertension	54 (62.8%)
Hypercholesterolemia	46 (53.5%)
Diabetes mellitus	28 (32.6%)
Left ventricular function	
Mild impairment (>50% LVEF ≥40%)	12 (14.0%)
Moderate impairment (LVEF 30-39%)	10 (11.6%)
Severe impairment (LVEF <30%)	1 (1.2%)
Antiarrhythmic drugs	
Class I	1 (1.2%)
Class II	59 (68.6%)
Class III	6 (7.0%)
Class IV	6 (7.0%)

BMI = body mass index; **iHD** = ischemic heart disease; **vHD** = valvular heart disease; **cHD** = combined heart disease; **AF** = atrial fibrillation; **LVEF** = left ventricular ejection fraction.

Table 2
EGM characteristics and endo-epicardial difference

EGM features	Endocardium	Epicardium	P-value
	Median [IQR]	Median [IQR]	
Median voltage (mV)	4.65 [3.15, 6.52]	7.01 [5.34, 8.35]	<0.001
LVA (%)	4.22 [1.71, 8.10]	2.86 [1.15, 5.93]	0.024
SP (%)	81.62 [73.14, 88.74]	83.31 [76.5, 88.73]	0.295
SDP (%)	8.87 [6.67, 12.42]	9.47 [6.96, 13.09]	0.523
LDP (%)	5.12 [3.15, 10.96]	3.98 [1.68, 7.53]	0.019
FP (%)	1.66 [0.63, 3.28]	1.33 [0.54, 2.98]	0.351
FD (ms)			
FD-SDP	9 [8, 10]	8 [6, 9]	<0.001
FD-LDP	20 [18, 24]	20 [18, 25]	0.808
FD-DP	12 [10, 16]	10 [7, 12]	<0.001
FD-FP	22 [16, 26]	20 [16, 27]	0.968

EGM = electrogram; **LVA** = low-voltage area; **SP** = single potentials; **SDP** = short double potentials; **LDP** = long double potentials; **FP** = fractionated potentials; **DP** = double potentials; **FD** = fractionation duration.

8.35] mV, P < 0.001). Correspondingly, the amount of LVAs was more frequently found at the endocardium (2.86 [1.15, 5.93] mV vs 4.22 [1.71, 8.10] mV, P = 0.024). The proportions of SP, SDP, and FP at the endocardium and epicardium also did not differ; only LDP were more often recorded at the endocardium (5.1 [3.2, 11.0] % vs 4.0 [1.7, 7.5] %, P = 0.019). The FD of SDP was longer at the endocardium (9 [8, 10] ms vs 8 [6, 9] ms, P < 0.001), whereas the FD of LDP and FP was comparable between both layers (LDP: 20 [18, 24] ms vs 20 [18, 25] ms, P = 0.808; FP: 22 [16, 26] ms vs 20 [16, 27] ms, P = 0.968).

In total, 9,474 (5.8%) areas of EEA were found in 83 (96.5%) patients. Fig. 1 illustrates the amount of EEA for each individual patient, which ranged from 0 to 25.8% (median: 3.0%).

3.3. Potential fractionation in relation to EEA

The upper panel of Fig. 2 shows typical examples of non-EEA and EEA areas; potentials recorded from various electrodes

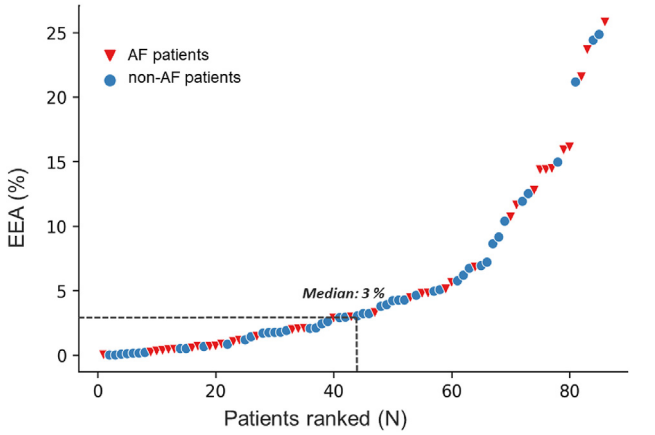

Figure 1. The amount of EEA is demonstrated for each individual patient; patients are ranked according to the increasing EEA (%). The median value of EEA (%) is marked using the median dot (3%).
EEA = endo-epicardial asynchrony

scattered across the mapping array are depicted outside the activation maps. In non-EEA areas, mainly SP were found in contrast to EEA areas from which mainly non-SP were recorded.

The lower panel of Fig. 2 illustrates the proportion of various types of potentials in all mapping areas with and without EEA at both the endo- and epicardium. At areas of EEA, particularly the proportions of LDP (endocardium: 5.5% vs 35.3%, epicardium: 3.5% vs 27.3%) and FP (endocardium: 1.9% vs 14.4%, epicardium: 1.6% vs 9.7%) increased, at the expense of the proportion of SP (endocardium: 82.9% vs 38.9%, epicardium: 84.3% vs 51.6%). Hence, the composition of all potential types in EEA and non-EEA regions differed significantly (P < 0.001).

3.4. Unipolar voltages in relation to EEA

Unipolar voltage distribution histograms in both non-EEA and EEA areas at the endocardium and epicardium are depicted in the upper panel of Fig. 3. At both layers, potential voltages in EEA areas were lower than in non-EEA areas (endocardium: 5.20 [2.81, 9.22] mV vs 1.56 [0.89, 2.7] mV, P < 0.001; epicardium: 7.38 [4.36, 10.61] mV vs 2.53 [1.15, 4.74] mV, P < 0.001), while the proportion of LVAs was higher in EEA areas (endocardium: 3.9% vs 29.8%, P < 0.001; epicardium: 2.8% vs 21.0%, P < 0.001).

3.5. Fractionation duration (FD) in relation to EEA

The middle and lower panel of Fig. 3 shows the relative frequency distribution histograms of the FD of DP and FP measured in EEA and non-EEA areas at the endocardium and epicardium separately. At both layers, the FD of DP and FP in EEA areas were increased compared to those in non-EEA areas (FD-DP: endocardium: 11 [7, 18] vs 20 [15, 28] ms, P < 0.001; epicardium: 9 [6, 14] vs 20 [13, 30] ms, FD-FP: endocardium: 20 [14, 27] vs 28 [21, 36] ms, P < 0.001; epicardium: 20 [15, 27] vs 26 [19, 39] ms).

3.6. Correlation between endo-epicardial unipolar potential characteristics

The relationships between endo- and epicardial potential characteristics are listed in Table 3. There was a strong correlation between the endo-epicardial proportion of LVAs (r = 0.753, P < 0.001), whereas there was a moderate correlation between

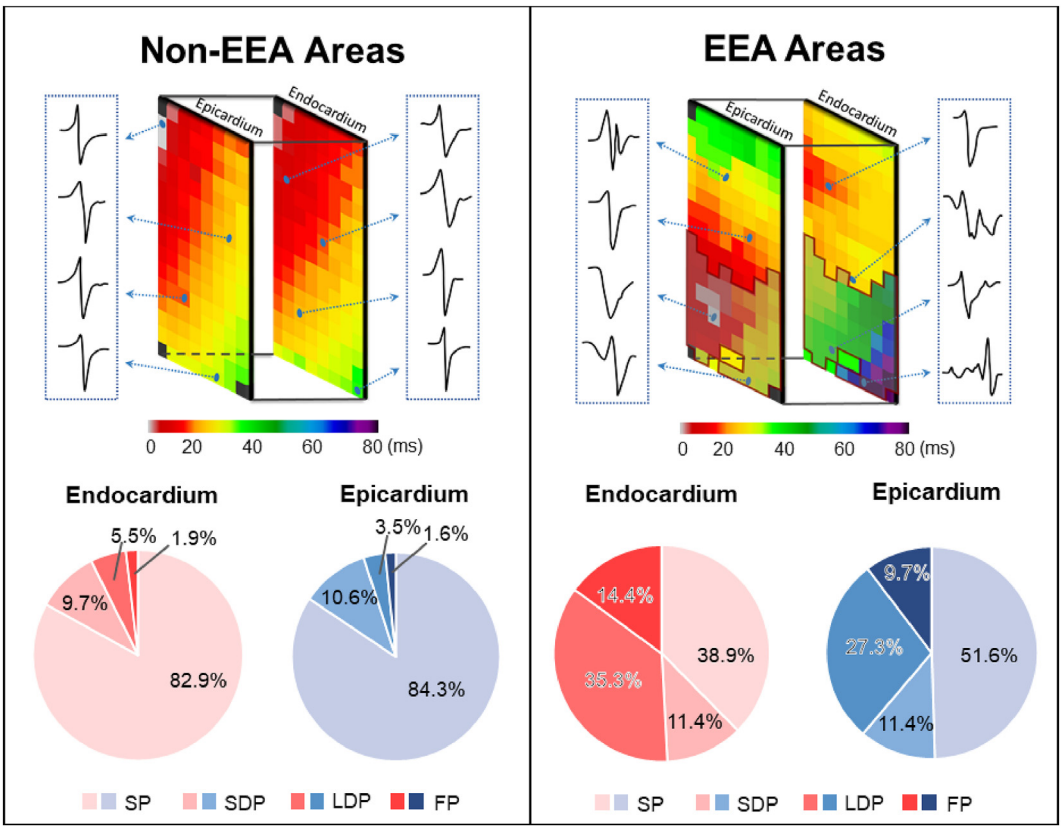

Figure 2. Representative examples of potential types and their proportion in the non-EEA areas and EEA areas. Upper panel: Two examples of activation maps depict non-EEA and EEA areas. EEA areas are marked with a scarlet red frame. Lower panel: The composition of potential types in non-EEA and EEA areas at the endocardium (red pies) and epicardium (blue pies)
SP = single potential, **SDP** = short double potential, **LDP** = long double potential, **FP** = fractionated potential, **EEA** = endo-epicardial asynchrony.

endo-epicardial potential voltages (r = 0.681, P < 0.001). With respect to the different potential types, only the amount of SP and LDP was strongly correlated (r = 0.749, r = 0.702, respectively, P < 0.001) between both layers. There were moderate correlations between endo-epicardial SDP and FP (r = 0.589, r = 0.603, respectively, P < 0.001). In addition, the FD of LDP was moderately correlated (r = 0.444, P < 0.001), whereas the FDs of SDP and FP were weakly correlated (r = 0.289, P = 0.007; r = 0.245, P = 0.023, respectively).

3.7. *Influence of AF episodes on unipolar potential characteristics in EEA areas*

Of the 9,474 EEA areas, 4,373 (11.4%) were found in patients with history of AF, while 5,101 (8.9%) sites were found in patients without AF (P < 0.001). As illustrated in Table 4, patients with AF had lower potential voltages in EEA areas at both the endocardium and epicardium (endocardium: 1.66 [0.89, 2.94] vs 1.48 [0.88, 2.45], P < 0.001; epicardium: 3.01 [1.34, 5.5] vs 2.15 [1.03, 3.82], P < 0.001) than patients without AF, whereas the proportion of LVAs in AF patients was higher at the epicardium only (no AF: 18.4% vs AF: 24.0%, P < 0.001). In addition, long FDs were found in patients with AF, with an exception of the FD of endocardial FP (28.0 [21.0, 37.0] vs 28.0 [21.0, 37.0], P = 0.972). A larger proportion of LDP was present at both layers in patients with AF (endocardium: 32.8% vs 39.5%; epicardium: 27.3 vs 29.6%), while these patients had a lower proportion of FP at the endocardium and a higher proportion at the epicardium. (endocardium: 16.4% vs 13.3%; epicardium: 7.7% vs 13.4%).

3.8. *Identification of potential characteristics predictive for EEA*

The outcomes of univariable and multivariable logistic regression analyses to determine appropriate EGM characteristics for predicting the degree of EEA are depicted in Table 5. Univariable logistic analysis was performed between the degree of EEA and all endocardial and epicardial potential characteristics. For both layers, all characteristics − except the proportion of SDP − were significantly associated with a higher degree of EEA.

Potential characteristics that were significantly related to EEA in univariable logistic regression were incorporated into multivariable regression models to establish the AFS. This resulted in an endocardial AFS (endo-AFS) containing the proportion of LVAs (OR: 1.644, 95% CI: 1.307-2.068, P <0.001) and SPs (OR: 0.916, 95% CI: 0.861-0.975, P = 0.006) and an epicardial AFS (epi-AFS) containing median voltages (OR: 0.647, 95% CI: 0.489-0.856, P = 0.002) and the proportion of LDP (OR: 1.185, 95% CI: 1.037-1.354, P = 0.012). For the AFS containing both endocardial and epicardial EGM characteristics (EE-AFS), the proportion of endocardial LVAs (OR: 1.728, 95% CI: 1.334-2.238, P < 0.001) and the FD of epicardial DP (OR: 1.305, 95% CI: 1.108-1.538, P = 0.001) were included. The endo-/epi-AFS and EE-AFS are illustrated in Fig. 4.

3.9. *Assessment of the Asynchrony Fingerprint Score (AFS)*

Fig. 5 demonstrates ROC curves of the accuracy of the endo-/epi-AFS and EE-AFS in estimating the degree of EEA. Although the EE-AFS showed the best predictive value (AUC: 0.913, 95% CI: 0.860-0.967), both the endo-AFS and epi-AFS also showed good

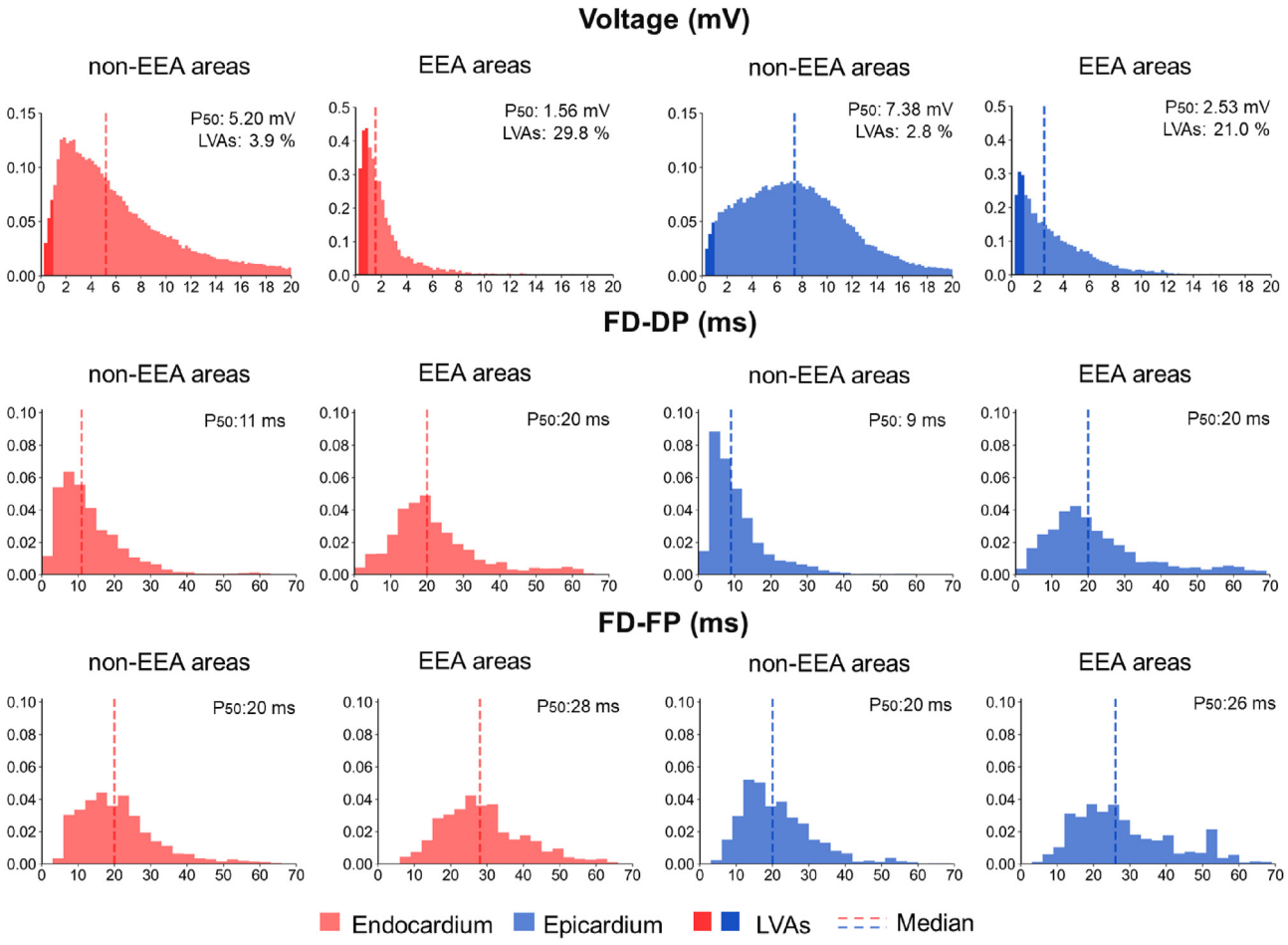

Figure 3. Histograms of the relative frequency distribution of voltages and FD in the non-EEA and EEA areas at the endocardium and epicardium. Red and blue colors represent endocardial and epicardial mapping data, respectively. In the upper panel, LVAs are highlighted by darker colors. Dashed lines indicate median values.
FD = fractionation duration, **DP** = double potential, **FP** = fractionated potential, **EEA** = endo-epicardial asynchrony, **LVAs** = low-voltage areas.

Table 3
The correlation of EGM characteristics between the endocardium and epicardium

	Median voltage (mV)	LVA (%)	SP (%)	SDP (%)	LDP (%)	FP (%)	FD-SDP (ms)	FD-LDP (ms)	FD-DP (ms)	FD-FP (ms)
Rho	0.681	0.753	0.749	0.589	0.702	0.603	0.245	0.444	0.475	0.289
P	<0.001	<0.001	<0.001	<0.001	<0.001	<0.001	0.023	<0.001	<0.001	0.007

EGM = electrogram; **LVA** = low-voltage area; **SP** = single potentials; **SDP** = short double potentials; **LDP** = long double potentials; **FP** = fractionated potentials; **DP** = double potentials; **FD** = fractionation duration.

discrimination with AUCs of 0.901 (95% CI: 0.840-0.962) and 0.830 (95% CI: 0.740-0.920), respectively.

Subsequently, the endo-AFS, epi-AFS, and EE-AFS were computed for each individual patient and illustrated in Fig. 6. EE-AFS has the best correlation with the amount of EEA per patient ($r = 0.813$, $P < 0.001$), although the endo-AFS and epi-AFS also have a good correlation ($r = 0.789$ and $r = 0.684$, respectively, $P < 0.001$ for both).

4. Discussion

4.1. Key findings

Simultaneous endo-epicardial SR mapping of the human RA demonstrated that both endocardial and epicardial areas of EEA are characterized by decreased potential voltages, an increase in the number of LDP and FP and prolongation of DP and FP durations. EE-AFS has the highest predictive value for identification of EEA and determining the amount of EEA. In addition, the AFS derived from solely the endo- or epicardium also has a good predictive value.

4.2. Endo-epicardial asynchrony

Discordant activation between the endocardium and epicardium was initially described in isolated canine atria by Schuessler et al.[3] in 1993 by performing simultaneous endo-epicardial mapping. They observed that EEA increased during atrial tachyarrhythmias compared to SR and also demonstrated that EEA was correlated with heterogeneity of the anatomical architecture of the RA, especially regions composed of pectinate muscles and cardiac

Table 4
Subgroup analysis of EGM characteristics in EEA areas

	Endocardium			Epicardium		
	Median [IQR]			Median [IQR]		
	non-AF	AF	P-value	non-AF	AF	P-value
Voltage (mV)	1.66 [0.89, 2.94]	1.48 [0.88, 2.45]	<0.001	3.01 [1.34, 5.5]	2.15 [1.03, 3.82]	<0.001
LVA (%)	29.2	30.6	0.289	18.4	24	<0.001
FD (ms)						
FD-DP	20.0 [14.0, 26.0]	20.0 [15.0, 31.0]	<0.001	18.0 [13.0, 26.0]	21.0 [15.0, 33.0]	<0.001
FD-FP	28.0 [21.0, 37.0]	28.0 [21.0, 37.0]	0.972	21.0 [15.0, 28.0]	30.5 [22.0, 42.0]	<0.001
Potential type (%)			<0.001			<0.001
SP	39.4	35.5		51.1	47.7	
SDP	11.5	11.8		13.8	9.2	
LDP	32.8	39.5		27.3	29.6	
FP	16.4	13.3		7.7	13.4	

EGM = electrogram; **EEA** = endo-epicardial asynchrony; **AF** = atrial fibrillation; LVA = low-voltage area; **SP** = single potentials; **SDP** = short double potentials; **LDP** = long double potentials; **FP** = fractionated potentials; **DP** = double potentials; **FD** = fractionation duration.

Table 5
Univariate and multivariate logistic regression analyses of EGM characteristics

Univariate logistic regression				
Endocardium				
	P	OR	95% CI	
Median voltage	<0.001	0.673	0.542	0.836
LVA	<0.001	1.623	1.314	2.004
SP%	0.001	0.927	0.885	0.971
SDP%	0.81	1.01	0.928	1.1
LDP%	<0.001	1.196	1.083	1.322
FP%	0.007	1.348	1.086	1.674
FD				
FD-SDP	0.01	1.351	1.073	1.701
FD-LDP	0.016	1.115	1.021	1.217
FD-DP	<0.001	1.314	1.151	1.501
FD-FP	0.011	1.071	1.015	1.129
Epicardium				
	P	OR	95% CI	
Median voltage	<0.001	0.597	0.457	0.78
LVA	<0.001	1.497	1.213	1.847
SP%	0.001	0.916	0.868	0.966
SDP%	0.249	1.047	0.968	1.133
LDP%	0.001	1.28	1.113	1.472
FP%	0.004	1.458	1.127	1.887
FD				
FD-SDP	0.013	1.38	1.071	1.78
FD-LDP	0.005	1.121	1.036	1.214
FD-DP	<0.001	1.251	1.095	1.429
FD-FP	0.036	1.049	1.003	1.097
Multivariate logistic regression				
Endocardium				
	P	OR	95% CI	
LVA	<.001	1.644	1.307	2.068
SP%	0.006	0.916	0.861	0.975
Epicardium				
	P	OR	95% CI	
Median voltage	0.002	0.647	0.489	0.856
LDP%	0.012	1.185	1.037	1.354
EE				
	P	OR	95% CI	
endo LVA	<.001	1.728	1.334	2.238
epi FD-DP	0.001	1.305	1.108	1.538

EGM = electrogram; **LVA** = low-voltage area; **SP** = single potentials; **SDP** = short double potentials; **LDP** = long double potentials; **FP** = fractionated potentials; **DP** = double potentials; **FD** = fractionation duration; **endo** = endocardial; **epi** = epicardial; **EE** = endo- and epicardium.

fibers with different alignments. Several studies revealed that the severity of EEA is associated with AF progression in animal models.[4-6] Our research group performed simultaneous high-resolution endo-epicardial in-vivo mapping and provided evidence of EEA occurring during AF in human LA and RA.[7,13] A recent endo-epicardial mapping study in the RA showed that during SR, EEA was more frequently present in patients with persistent AF than in patients without AF.[8] These observations indicate that the presence of EEA may be determined not only by the underlying anatomy but also by pathological alterations of the tissue structure. This hypothesis is further supported by the results of the present study demonstrating clear differences in EGM characteristics derived from non- EEA and EEA areas. By comparing the EGM characteristics of EEA areas in patients with and without AF, we found that EEA areas in patients with AF were characterized by lower potential voltages, longer FD-DP, and a higher proportion of LDPs at both the endo- and epicardium. However, the proportion of low-voltage potentials and FD-FP in the endocardial EEA areas of patients with AF was similar to that in patients without AF. This may be because, in the remodeled atrial areas, the loss of endo-epicardial coupling caused by structural remodeling, particularly at the epicardium, may facilitate the development of an arrhythmogenic substrate, which resulted in EEA.[14] In addition, a growing amount of evidence indicates that inflammation plays a role in promoting both structural and electrical remodeling of the atria. These remodeling processes involve atrial fibrosis, the modulation of gap junctions, and abnormalities in intracellular calcium handling.[15-18] Ryu et al.[19] demonstrated a transmural gradient in Cx40 and Cx43 expression and a loss of epicardial myocytes in response to epicardial inflammation may provide the substrate for the abnormal atrial conduction including EEA. Further studies are needed to reveal the direct effect of inflammation on EEA.

4.3. EEA and unipolar voltages

In this study, endocardial unipolar potential voltages were considerably lower than epicardial potential voltages and therefore, consequently, also a higher amount of LVAs was found at the endocardium. This finding is in line with previous mapping studies performed in atria.[9,10,15] This may be attributed to the complex atrial structure which, particularly at the endocardium, contains a complex network of myocardial fibers. Irregular endocardial surfaces due to varying diameters of pectinate muscles, the presence of a thick and anisotropic terminal crest and branching of myocardial fibers may cause source-sink mismatches. Hence, conduction disorders and low voltage, fractionated potentials develop. In addition,

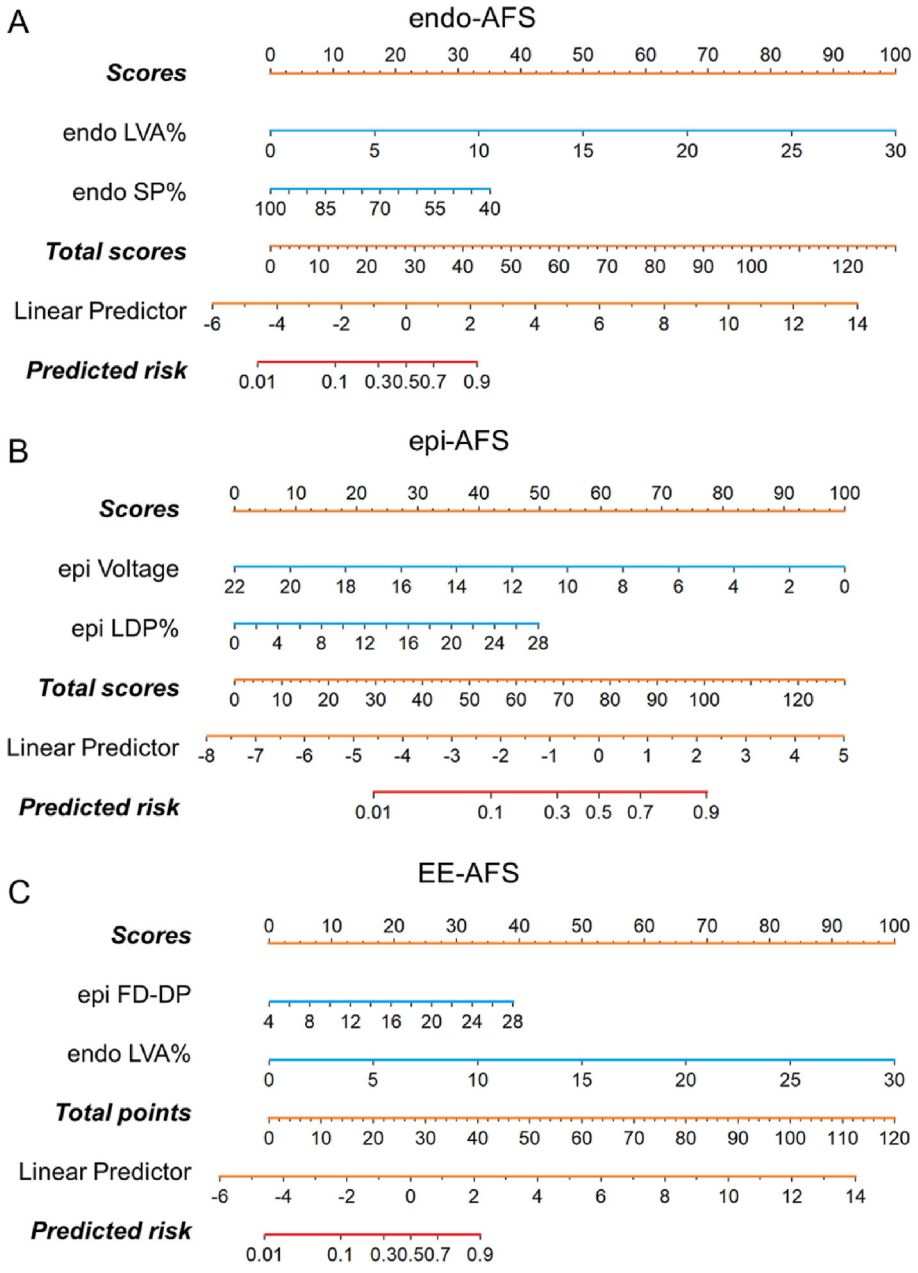

Figure 4. Three types of AFS for quantifying the severity of EEA in the RA obtained from the endocardium and/or epicardium. **A.** endo-AFS. A nomogram was established using the endocardial amount of LVAs and SPs. **B.** epi-AFS. A nomogram was established using unipolar potential voltages and amount of LDPs. **C.** EE-AFS. A nomogram was established using epicardial FD-DP and endocardial amount of LVAs. The first row ('scores') is used as a scale to calculate the corresponding scores for each variable, resulting in total scores for each patient, which can be used to determine the predicted risk based on the row of the total scores.
AFS = Asynchrony Fingerprinting Score, **EEA** = endo-epicardial asynchrony, **LDP** = long double potential, **SP** = single potential, **FD** = fractionation duration, **LVAs** = low-voltage areas.

lack of good contact between the electrodes and atrial tissue, which occurs mainly at the endocardium, could potentially explain the observed endo-epicardial potential voltage differences. In addition, lower unipolar potential voltages were found in EEA areas at both the endo- and epicardium. LVAs were also more pronounced in EEA areas; even up to 29.8% at the endocardium. As potential voltage depends on e.g. catheter design, myocardial fiber orientation and cycle length, any chosen LVA-threshold remains questionable. In the literature, different cut-off values have been used, depending on e.g. the mapping system and patient features.[11] However, as endo- and epicardial potential voltages and the amount of LVAs were included in the endo-/epi- and EE-AFS; potential voltage characteristics from both layers are good indicators of the presence of areas of EEA. A previous high-resolution epicardial mapping study performed in a cohort of 67 patients showed that during SR, patients with a history of AF are characterized by lower potential voltages compared to patients without AF.[12] Recently, Van Schie et al.[20] studied the relationship between endo-epicardial voltages and their predictive potential for LVAs. They showed that unipolar and omnipolar LVAs are frequently located exclusively at either the endo- or epicardium. Therefore, a combined endo-epicardial mapping approach was proposed to accurately identify dual-layer LVAs. Numerous other studies suggested that LVAs, whether unipolar or bipolar, are considered surrogate markers for the presence

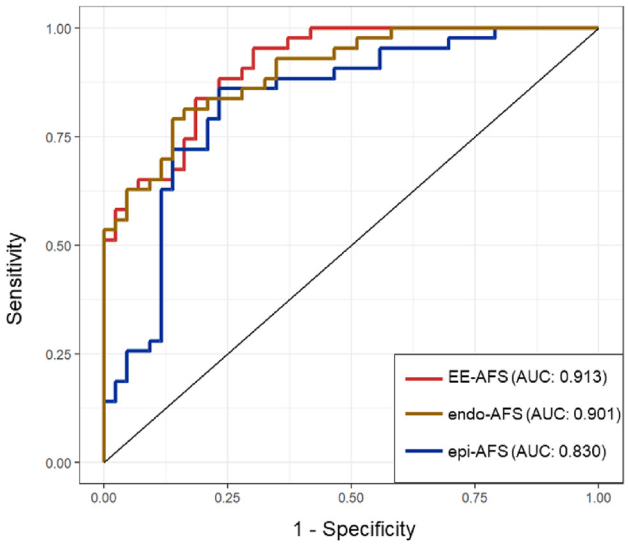

Figure 5. ROC of the three types of AFS. The red, yellow and blue lines represent EE-AFS, endo-AFS and epi-AFS, respectively. AUCs are depicted in the lower right box. **AFS** = Asynchrony Fingerprinting Score, **endo-AFS** = endocardial Asynchrony Fingerprinting Score, **epi-AFS** = epicardial Asynchrony Fingerprinting Score, **EE-AFS** = endo- and epicardial Asynchrony Fingerprinting Score.

of local fibrotic tissue.[21,22] In addition, the existence and extensiveness of LVAs have been shown to be a powerful predictor of arrhythmia recurrence.[23,24] We now demonstrated that decreased unipolar potential voltages are indicative of EEA areas and could also be used to estimate the amount of EEA during SR.

4.4. EEA and fractionated EGMs

Fractionated EGMs are mainly regarded as a combination of multiple electrical signals caused by the asynchronous activation of adjacent cardiomyocytes.[25] Several studies have shown that the clinical beneficial effect of ablation targeting complex fractionated atrial electrograms (CFAEs) is still controversial as CFAEs may have multiple causes of both pathologic and non-pathologic origin.[26-28] Fractionation of EGMs can be either physiological or pathological in nature caused by structural or cellular barriers. Pathological factors include e.g. collagen deposition, which separates adjacent myocardial cells giving rise to intra-atrial inhomogeneous conduction, including conduction block and/or EEA.[29-32] The resulting asynchronous activation of atrial tissue causes the fractionation of potentials. Previous simultaneous endo-epicardial mapping studies demonstrated that the fractionation of unipolar EGMs during SR can be attributed to asynchronous activation of the endo- and epicardial wall[9], whereas bipolar EGMs demonstrated to be less ideal for the detection of EEA.[10] By further investigating the relationship between fractionated EGMs and EEA using unipolar EGMs, we demonstrated for the first time that LDPs are most often linked to EEA in comparison to SDP and FP. In addition, particularly fractionated EGMs with lower potential voltages and prolonged FD are recorded from EEA areas. Our results showed that the LDP and FD of DP were the most sensitive potential characteristics to detect EEA within the atrial wall during SR, indicating the presence of extensive intramural conduction block resulting in EEA.

4.5. Clinical implications

In previous experimental and clinical mapping studies, it has been demonstrated that EEA may contribute to the perpetuation of AF. In the current study, we performed simultaneous endo-epicardial high-resolution mapping of the human right atrium and demonstrated that EEA areas are characterized by lower potential voltages and a higher number of fractionated potentials. These features may aid in identifying EEA areas that may be potential targets for AF therapy. Moreover, three different types of AFS were created (endo-/epi-AFS and EE-AFS) for identifying and determining the degree of EEA. Not surprisingly, EE-AFS has the most accurate predictive value compared to the single-layer AFS as it contains more information from both atrial layers. Nevertheless, the three different AFS showed good performance for predicting EEA. This indicates that AFS might be a potential diagnostic tool to classify patients according to the severity of EEA and enables a more personalized AF ablation strategy. As both single-layer AFS could also be used, the degree of EEA can be estimated by performing either endo- or epicardial mapping alone.

4.6. Limitations

Only limited areas of the RA free wall and the left atrium was not studied due to the risk of air embolisms. Given the association

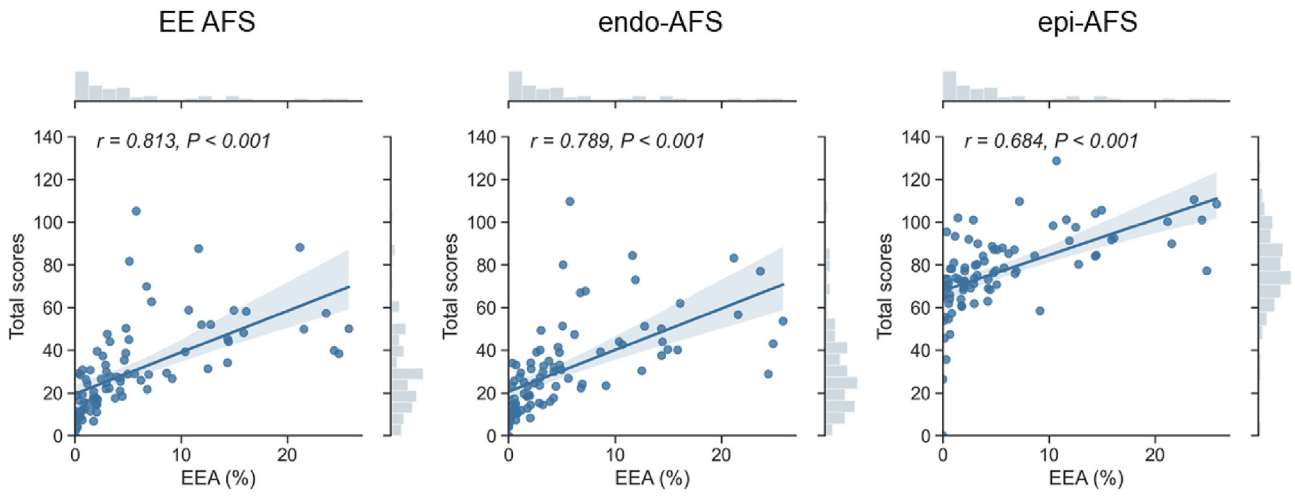

Figure 6. Correlation plot of the total scores calculated by the three different types of AFS (EE-, endo- and epi-AFS) and the amount of EEA (%). **AFS** = Asynchrony Fingerprinting Score, **EEA** = endo-epicardial asynchrony, **endo-AFS** = endocardial Asynchrony Fingerprinting Score, **epi-AFS** = epicardial Asynchrony Fingerprinting Score, **EE-AFS** = endo- and epicardial Asynchrony Fingerprinting Score.

between EEA and AF, future studies should validate the proposed AFS in the left atrium.

5. Conclusions

In human RA, areas of EEA are mainly characterized by decreased potential voltages, an increase in the number of LDP and FP and the prolongation of DP and FP durations. The amount of EEA areas can be most accurately determined by the EE-AFS, incorporating epicardial FD-DP and the amount of endocardial LVAs or the AFS derived solely from the endo- or epicardium. Therefore, AFS, as a novel approach using integrated data from the endo- and/or epicardium, may enable the precise determination of the amount of EEA, including potential AF-related arrhythmogenic substrates.

Sources of funding

N.M.S. de Groot, MD, PhD is supported by funding grants from NWO-Vidi (Grant No. 91717339), Biosense Webster Inc (USA) (ICD783454) and Medical Delta (Delft, the Netherlands).

Data availability

The data underlying this article will be shared on reasonable request to the corresponding author.

Conflict of interest

The authors have no conflict of interest.

Disclosures

None.

Acknowledgements

The authors would like to thank A.J.J.C. Bogers, J.A. Bekkers; C. Kik; W.J. Van Leeuwen; F.B.S. Oei; P.C. Van de Woestijne; F.R.N. van Schaagen; L.N. Van Staveren; A. Heida; M.C. Roos-Serote; R.K. Kharbanda; C. Li; C. Zhang; Z. Ye; J.H. Amesz; N.L. Ramdat Misier; R.D. Zwijnenburg; L. Pool; M.F.A. Bierhuizen for their contribution to this work.

Appendix A. Supplementary data

Supplementary data to this article can be found online at https://doi.org/10.1016/j.hjc.2023.07.006.

References

1. de Groot NM, Houben RP, Smeets JL, et al. Electropathological substrate of longstanding persistent atrial fibrillation in patients with structural heart disease: epicardial breakthrough. *Circulation*. 2010;122:1674–1682. doi: CIRCULATIONAHA.109.910901 [pii] 10.1161/CIRCULATIONAHA.109.910901.
2. Hansen BJ, Zhao J, Csepe TA, et al. Atrial fibrillation driven by micro-anatomic intramural re-entry revealed by simultaneous sub-epicardial and sub-endocardial optical mapping in explanted human hearts. *Eur Heart J*. 2015;36:2390–2401. https://doi.org/10.1093/eurheartj/ehv233.
3. Schuessler RB, Kawamoto T, Hand DE, et al. Simultaneous epicardial and endocardial activation sequence mapping in the isolated canine right atrium. *Circulation*. 1993;88:250–263. https://doi.org/10.1161/01.cir.88.1.250.
4. Everett THt, Wilson EE, Hulley GS, Olgin JE. Transmural characteristics of atrial fibrillation in canine models of structural and electrical atrial remodeling assessed by simultaneous epicardial and endocardial mapping. *Heart Rhythm*. 2010;7:506–517. https://doi.org/10.1016/j.hrthm.2009.12.030.
5. Eckstein J, Maesen B, Linz D, et al. Time course and mechanisms of endo-epicardial electrical dissociation during atrial fibrillation in the goat. *Cardiovasc Res*. 2011;89:816–824. https://doi.org/10.1093/cvr/cvq336.
6. Eckstein J, Zeemering S, Linz D, et al. Transmural conduction is the predominant mechanism of breakthrough during atrial fibrillation: evidence from simultaneous endo-epicardial high-density activation mapping. *Circ Arrhythm Electrophysiol*. 2013;6:334–341. doi: CIRCEP.113.000342 [pii] 10.1161/CIRCEP.113.000342.
7. de Groot N, van der Does L, Yaksh A, et al. Direct Proof of Endo-Epicardial Asynchrony of the Atrial Wall During Atrial Fibrillation in Humans. *Circ Arrhythm Electrophysiol*. 2016;9. doi: CIRCEP.115.003648[pii]10.1161/CIRCEP.115.003648.
8. Kharbanda RK, Knops P, van der Does L, et al. Simultaneous Endo-Epicardial Mapping of the Human Right Atrium: Unraveling Atrial Excitation. *J Am Heart Assoc*. 2020;9:e017069. https://doi.org/10.1161/JAHA.120.017069.
9. van der Does L, Knops P, Teuwen CP, et al. Unipolar atrial electrogram morphology from an epicardial and endocardial perspective. *Heart Rhythm*. 2018;15:879–887. doi: S1547-5271(18)30130-9 [pii]10.1016/j.hrthm.2018.02.020.
10. van der Does L, Starreveld R, Kharbanda RK, et al. Detection of Endo-epicardial Asynchrony in the Atrial Wall Using One-Sided Unipolar and Bipolar Electrograms. *J Cardiovasc Transl Res*. 2021;14:902–911. doi: 10.1007/s12265-021-10111-1 10.1007/s12265-021-10111-1[pii].
11. de Groot NMS, Shah D, Boyle PM, et al. Critical appraisal of technologies to assess electrical activity during atrial fibrillation: a position paper from the European Heart Rhythm Association and European Society of Cardiology Working Group on eCardiology in collaboration with the Heart Rhythm Society, Asia Pacific Heart Rhythm Society, Latin American Heart Rhythm Society and Computing in Cardiology. *Europace*. 2021. doi: 6456176[pii]10.1093/europace/euab254.
12. van Schie MS, Starreveld R, Bogers A, de Groot NMS. Sinus rhythm voltage fingerprinting in patients with mitral valve disease using a high-density epicardial mapping approach. *Europace*. 2021;23:469–478. doi: 6085831[pii]10.1093/europace/euaa336.
13. Kharbanda RK, Kik C, Knops P, Bogers A, de Groot NMS. First Evidence of Endo-Epicardial Asynchrony of the Left Atrial Wall in Humans. *JACC Case Rep*. 2020;2:745–749. https://doi.org/10.1016/j.jaccas.2020.02.027S2666-0849(20)30354-30355[pii].
14. Maesen B, Zeemering S, Afonso C, et al. Rearrangement of atrial bundle architecture and consequent changes in anisotropy of conduction constitute the 3-dimensional substrate for atrial fibrillation. *Circ Arrhythm Electrophysiol*. 2013;6:967–975. doi: CIRCEP.113.000050[pii]10.1161/CIRCEP.113.000050.
15. Saba S, Janczewski AM, Baker LC, et al. Atrial contractile dysfunction, fibrosis, and arrhythmias in a mouse model of cardiomyopathy secondary to cardiac-specific overexpression of tumor necrosis factor-alpha. *Am J Physiol Heart Circ Physiol*. 2005;289:H1456–H1467. https://doi.org/10.1152/ajpheart.00733.2004.
16. Liew R, Khairunnisa K, Gu Y, et al. Role of tumor necrosis factor-alpha in the pathogenesis of atrial fibrosis and development of an arrhythmogenic substrate. *Circ J*. 2013;77:1171–1179. https://doi.org/10.1253/circj.cj-12-1155.
17. Baum JR, Long B, Cabo C, Duffy HS. Myofibroblasts cause heterogeneous Cx43 reduction and are unlikely to be coupled to myocytes in the healing canine infarct. *Am J Physiol Heart Circ Physiol*. 2012;302:H790–H800. https://doi.org/10.1152/ajpheart.00498.2011.
18. Nattel S, Burstein B, Dobrev D. Atrial remodeling and atrial fibrillation: mechanisms and implications. *Circ Arrhythm Electrophysiol*. 2008;1:62–73. https://doi.org/10.1161/CIRCEP.107.754564.
19. Ryu K, Li L, Khrestian CM, et al. Effects of sterile pericarditis on connexins 40 and 43 in the atria: correlation with abnormal conduction and atrial arrhythmias. *Am J Physiol Heart Circ Physiol*. 2007;293:H1231–H1241. https://doi.org/10.1152/ajpheart.00607.2006.
20. Van Schie MS, Knops P, Zhang L, Van Schaagen FRN, Taverne Y, De Groot NMS. Detection of endo-epicardial atrial low-voltage areas using unipolar and omnipolar voltage mapping. *Front Physiol*. 2022;13:1030025. doi: 1030025[pii]10.3389/fphys.2022.1030025.
21. Huo Y, Gaspar T, Pohl M, et al. Prevalence and predictors of low voltage zones in the left atrium in patients with atrial fibrillation. *Europace*. 2018;20:956–962. https://doi.org/10.1093/europace/eux082.
22. Blandino A, Bianchi F, Grossi S, et al. Left Atrial Substrate Modification Targeting Low-Voltage Areas for Catheter Ablation of Atrial Fibrillation: A Systematic Review and Meta-Analysis. *Pacing Clin Electrophysiol*. 2017;40:199–212. https://doi.org/10.1111/pace.13015.
23. Rolf S, Kircher S, Arya A, et al. Tailored atrial substrate modification based on low-voltage areas in catheter ablation of atrial fibrillation. *Circ Arrhythm Electrophysiol*. 2014;7:825–833. doi: CIRCEP.113.001251[pii]10.1161/CIRCEP.113.001251.
24. Yang G, Yang B, Wei Y, et al. Catheter Ablation of Nonparoxysmal Atrial Fibrillation Using Electrophysiologically Guided Substrate Modification During Sinus Rhythm After Pulmonary Vein Isolation. *Circ Arrhythm Electrophysiol*. 2016;9:e003382. doi: CIRCEP.115.003382[pii] 10.1161/CIRCEP.115.003382.
25. Narayan SM, Wright M, Derval N, et al. Classifying fractionated electrograms in human atrial fibrillation using monophasic action potentials and activation mapping: evidence for localized drivers, rate acceleration, and nonlocal signal etiologies. *Heart Rhythm*. 2011;8:244–253. https://doi.org/10.1016/j.hrthm.2010.10.020.
26. Providencia R, Lambiase PD, Srinivasan N, et al. Is There Still a Role for Complex Fractionated Atrial Electrogram Ablation in Addition to Pulmonary Vein Isolation in Patients With Paroxysmal and Persistent Atrial Fibrillation? Meta-

Analysis of 1415 Patients. *Circ Arrhythm Electrophysiol*. 2015;8:1017–1029. https://doi.org/10.1161/CIRCEP.115.003019.
27. Verma A, Jiang CY, Betts TR, et al. Approaches to catheter ablation for persistent atrial fibrillation. *N Engl J Med*. 2015;372:1812–1822. https://doi.org/10.1056/NEJMoa1408288.
28. Calvert P, Lip GYH, Gupta D. Radiofrequency catheter ablation of atrial fibrillation: A review of techniques. *Trends Cardiovasc Med*. 2022. https://doi.org/10.1016/j.tcm.2022.04.002.
29. Kostin S, Klein G, Szalay Z, Hein S, Bauer EP, Schaper J. Structural correlate of atrial fibrillation in human patients. *Cardiovasc Res*. 2002;54:361–379. https://doi.org/10.1016/s0008-6363(02)00273-0.
30. Gaudesius G, Miragoli M, Thomas SP, Rohr S. Coupling of cardiac electrical activity over extended distances by fibroblasts of cardiac origin. *Circ Res*. 2003;93:421–428. https://doi.org/10.1161/01.RES.0000089258.40661.0C.
31. de Bakker JM, Wittkampf FH. The pathophysiologic basis of fractionated and complex electrograms and the impact of recording techniques on their detection and interpretation. *Circ Arrhythm Electrophysiol*. 2010;3:204–213. doi: 3/2/204[pii]10.1161/CIRCEP.109.904763.
32. Gardner PI, Ursell PC, Fenoglio Jr JJ, Wit AL. Electrophysiologic and anatomic basis for fractionated electrograms recorded from healed myocardial infarcts. *Circulation*. 1985;72:596–611. https://doi.org/10.1161/01.cir.72.3.596.